Biosensors and Bioelectronics 130 (2019) 139–146

Contents lists available at ScienceDirect

Biosensors and Bioelectronics

journal homepage: www.elsevier.com/locate/bios

Microchip electrophoresis based aptasensor for multiplexed detection of antibiotics in foods via a stir-bar assisted multi-arm junctions recycling for signal amplification

Kai Zhang[a,b], Ning Gan[a,*], Zhipeng Shen[a], Jinxuan Cao[b,*], Futao Hu[b], Tianhua Li[a]

[a] Faculty of Material Science and Chemical Engineering, Ningbo University, Ningbo 315211, China
[b] Key Laboratory of Animal Protein Food Processing Technology of Zhejiang Province, Ningbo University, Ningbo 315211, China

ARTICLE INFO

Keywords:
Multiplexed detection
Aptasensor
Microchip electrophoresis
Stir-bar
Multi-arm junctions recycling
Antibiotics detection

ABSTRACT

Microchip electrophoresis (MCE) was a good available method for high-throughput and rapid detecting chemical pollutants in food samples. However, many of the reported MCE assays involve complex design of microchip, laborious operation and poor universality which limited its promotion in multiple antibiotics' detection. Herein, a multiplexed aptasensor was developed based on a universal double-T type microchip to one-step and simultaneously detect several antibiotics within 3 min using chloramphenicol (CAP) and kanamycin (Kana) as representatives. Besides, a novel stir-bar assisted DNA multi-arm junctions recycling (MAJR) strategy was designed for transducing and amplifying the signal. The brief detection mechanism was as following: the added CAP and Kana can specifically react with their aptamer probes on the stir-bar and produce different single-stranded DNA primer, respectively. Afterwards, the primers can trigger MAJR to form a lot of three- and four-arm DNA junctions corresponding to different targets. The DNA multi-arm junctions can be easily separated and detected by MCE for quantification. Moreover, the stir-bar can facilitate phase separation and obviously eliminate matrix interference in food. The assay was successfully applied in milk and fish samples, showing excellent selectivity and sensitivity with a detection limits of 0.52 pg mL^{-1} CAP and 0.41 pg mL^{-1} Kana (S/N = 3). Thus, the assay holds a great potential application for screening of antibiotics in food.

1. Introduction

Antibiotics abuse can bring serious threats to human health, while many kinds of antibiotics maybe coexist in one food sample (Conzuelo et al., 2013; Gaudin, 2017; Oertel et al., 2004). Therefore, it is particularly desirable to simultaneously detect various antibiotics residues in one sample, enabling a rapid and robust quantification. The technique of microchip electrophoresis (MCE) was firstly developed by Ciba Geigy scientists in 1990s (Manz et al., 1990). During the last decade, microfluidic chip electrophoresis assay has aroused much attention because it have many superior advantages such as high throughput and separation efficiency (e.g. DNA, RNA, protein and so on) (Nantana et al., 2015; Spindel and Sapsford, 2014). MCE has been exploited for many fields such as medical diagnosis (Ye et al., 2010), pharmaceutical analysis (Shih et al., 2018), food safety (Martín et al., 2012). Nevertheless, there were few reported about detecting different categories of antibiotic residues using one MCE chip. The reasons are due to that the assay suffers from some of the following limitations. Firstly, because the molecule structure and electrical properties of different categories of antibiotics (normally 8 categories) are vary greatly. Their separation and detection conditions in electrophoresis are very different. Thus, a specially designed chip is needed to detect specific target (Lili et al., 2012). Secondly, most of multiplexed MCE systems require to fabricate complex microchannel networks and a large amount of valve actuation paths (Dincer et al., 2017; Suárez et al., 2009). All these limit its large-scale application. Thirdly, the sensitivity of MCE systems is normally limited since the low sample consumption (García and Henry, 2003; Lu et al., 2009). Therefore, all the above defects limit MCE's application in multiplexed antibiotics detection in food.

To develop universal multiplexed antibiotics detection strategy based on MCE, the signal transduction strategies are necessary. Recently, our group has designed some signal conversion strategies to transducer antibiotic molecules into various lengths of DNA fragments using encoded aptamer probes (Y. Wang et al., 2017; Zhou et al., 2018a, 2018b). An aptamer is a DNA or RNA strand with a certain sequence and shows special recognition ability to target molecules (Ellington and

* Corresponding authors.
E-mail addresses: ganning@nbu.edu.cn (N. Gan), caojinxuan@nbu.edu.cn (J. Cao).

https://doi.org/10.1016/j.bios.2019.01.044
Received 14 November 2018; Received in revised form 4 January 2019; Accepted 18 January 2019
Available online 29 January 2019
0956-5663/

Szostak, 1990; Tuerk and Gold, 1990). One of the advantages in these MCE strategies is to solve the difficulties of analyzing different categories of antibiotics on the same MCE platform. However, there were also some shortcomings in the above study. One main issue was expensive enzyme or time-consuming DNA amplified procedures. The enzymatic signal amplify strategy can be easily suffer from environmental factors, e.g. pH, temperature and ion concentration (Sun et al., 2016).

The enzyme-free signal amplification strategy based on DNA toehold-mediated strand-displacement reactions was widely used to fabricate high sensitive aptasensors (Gao et al., 2015; Yang et al., 2017). However, both of them suffer intrinsic limitation of signal leakage in which the hairpins could be opened each other in the absence of target (B. Wang et al., 2017). It can bring false positive results. The DNA multi-arm junctions recycling (MAJR) with a high-energy barrier was recently exploited to minimize signal leakage (Kotani and Hughes, 2017). A typical MAJR strategy contained three or four metastable DNA hairpin probes and the corresponding trigger probes. The hairpins include a stem of 12–18 pairs and a sticky end of 6–12 pairs (Bi et al., 2015; Wen et al., 2016; Zhihe et al., 2014). The complementary relationships between the hairpins are specified. In the presence of the trigger, a cascade of assembly steps with the hairpins can occur to from a large amount of three or four-arm branched junctions. Notably, the charge-to-mass ratio of three- and four-DNA branched junctions is different. Therefore, they can be easily separated and detected by MCE. Based on the above issues, we hoped to design encoded DNA probes to capture targets for signal conversion then trigger MAJR for signal amplification.

Herein, a high sensitivity, enzyme-free and universal MCE method was developed to simultaneously detect antibiotics using stir-bar assisted MAJR for signal amplification. The bar modified with encoded aptamer probes was employed to specially capture different target antibiotics, with CAP and Kana as model molecules. The principle is illustrated in Scheme 1. The assay exhibits several advantages. Firstly, the gold bar with encoded aptamer probes can enable signal conversion and facilitate phase separation to eliminate the matrix interference. Secondly, non-enzymatic MAJR was employed to amplify DNA fragments and realize multiplex detection. Thirdly, the conventional and commercialized microfluidic chip with portable LED induced fluorescence detector was employed for detection. It was robust and can be reused for 3000–4000 times. The assay was testified in several food samples, e.g. fish and milk samples.

2. Experiment

2.1. Reagents and apparatus

The sequences of oligonucleotide used in this strategy are shown in Table S1 and obtained from Shanghai Sangon Biological Engineering Technology & Services Co., Ltd (Shanghai, China). The kanamycin (Kana), gentamicin sulfate (GS), chloramphenicol (CAP), chlortetracycline (CTC), streptomycin (SM) and doxycycline (DOX) were purchased from company Sigma (USA). Kana-ELISA kit was supplied by Huaan Magnech Bio-tech (Beijing, China). $HAuCl_4$ was purchased from Aladdin (Shanghai, China). (3-mercaptopropyl)-tri-methoxysilane (MPTMS) tris(2-carboxyethyl), phosphine hydrochloride (TCEP) were purchased from Sigma-Aldrich Co., Ltd (Milan, Italy). Phosphate buffered saline (PBS, pH 7.4 contained 0.15 M NaCl, 0.1 M NaH_2PO_4, 0.1 M Na_2HPO_4) was prepared by standard methods. Double-distilled water was used throughout the study.

The transmission electron microscopic (TEM) image was acquired from a H600 transmission electron microscope (Hitachi, Japan). Scanning electron micrographs (SEM) was obtained from a S3400 N scanning electron microscope (Hitachi, Japan). MultiNA 202 System was purchased from Shimadzu. (Kyoto, Japan). Dynamic Light Scattering (DLS) was performed using a Zetasizer Nano ZS90 (Malvin Instruments, Ltd., Malvin, UK). Microplate reader (KHB ST-360) was purchased from Shanghai Kehua Bio-engineering Co. Ltd (Shanghai, China). The UV–vis spectra were recorded by a UV-1800 spectrophotometer from Shimazu Co. Ltd (Kyoto, Japan).

2.2. Synthesis of gold nanoparticles (AuNPs) modified stir-bar

The synthesis of AuNPs was referenced the previous reported (Song et al., 2011). The AuNPs modified gold bar was synthesized by our previous report (Zhang et al., 2018). In brief, a gold bar (99.99%, 10.0 cm in length and 0.2 mm in diameter) was placed to 1 mL of fresh MPTMS sol-gel (preparation details in the Supporting information) for 40 min at 25 °C. Then, pou out the bar and wish above three times with double-distilled water. Next, the bar was placed in 2 mL of AuNPs solution (2 nM) overnight at 4 °C to obtain the AuNPs modified gold bar. It was stored in PBS buffer (pH = 7.4) for further use.

2.3. Preparation of aptamer probe labeled gold stir-bar

This protocol was based on the Au-S interaction between the gold lattice and thiolated primers. The DNA probes were heated to 95 °C for 5 min and then gradually cooled to room temperature for 2 h and stored in 4 °C. In order to ensure the desirable secondary structures, the 12.5 mM of $MgCl_2$ was supplemented in above mixture before using (Bi et al., 2015). Firstly, 80 μL of 10 mM TCEP placed in 80 μL of 10 μM thiol DNA probes of primer 1 and primer 2, and reacted 1 h at 25 °C to active thiol group. Then 1740 μL PBS buffer was added to the solution. Next, the stir-bar was immersed in the above mixture overnight at 4 °C. Then, the stir-bar was taken out and washed for three times with double-distilled water to remove uncombined primers. Next, the stir-bar was placed into 2 mL PBS buffer which contained 2 μM Kana-apt and CAP-apt respectively for 1 h at 25 °C. Finally, the composite of DNA probes functionalized gold stir-bar was washed three times with double-distilled water and stored in PBS buffer at 4 °C for further use.

2.4. Instrumental parameters of the MCE system

The MultiNA 202 system was equipped with a commercially double-T shape microchip (length: 3.5 cm and width: 2.3 cm) for separation of samples, and a blue LED (470 nm; 20 mA) detector for samples' detection at 525 nm. The configuration and microchannel parameters of the double-T microchip are shown in Fig. S1. Moreover, the voltage used for the MCE separation was described in Table S2. The system operation, data collection and analysis were automatically operated by a laptop.

2.5. Preparation of aptasensor detected CAP and Kana using MCE system

At first, the gold bar coating with numerous capture probes was immersed in 2 mL PBS buffer (pH = 7.4, 10 nM) which contained different concentrations of Kana and CAP at 25 °C for 1 h. After a completion of reaction, the gold bar was taken out, washed three times with deionized water. Next, the bar was placed into a new 2 mL of PBS buffer (pH = 7.4, 10 nM). The buffer contained 0.4 μM hairpins (H1, H2, H3, H4, H5, H6 and H7). Then, 50 μL of reaction solution was on-line labeled by 1 μL fluorescent dye (Lot # 1683656, 50× SYBR Gold). Finally, about 150 pL of mixture solution was automatically injected into MCE for detection. The SYBR Gold can combined with dsDNA and ssDNA to excite fluorescence signal (excitation/emission: 470/525 nm). The produce of three- and four-arm DNA junctions which combined SYBR Gold dye migrated to the LED detector to generate fluorescence signal and transferred to detection system for quantification.

2.6. Detection of CAP and Kana in actual milk and fish samples

Fresh milk and fish samples were purchased from the local

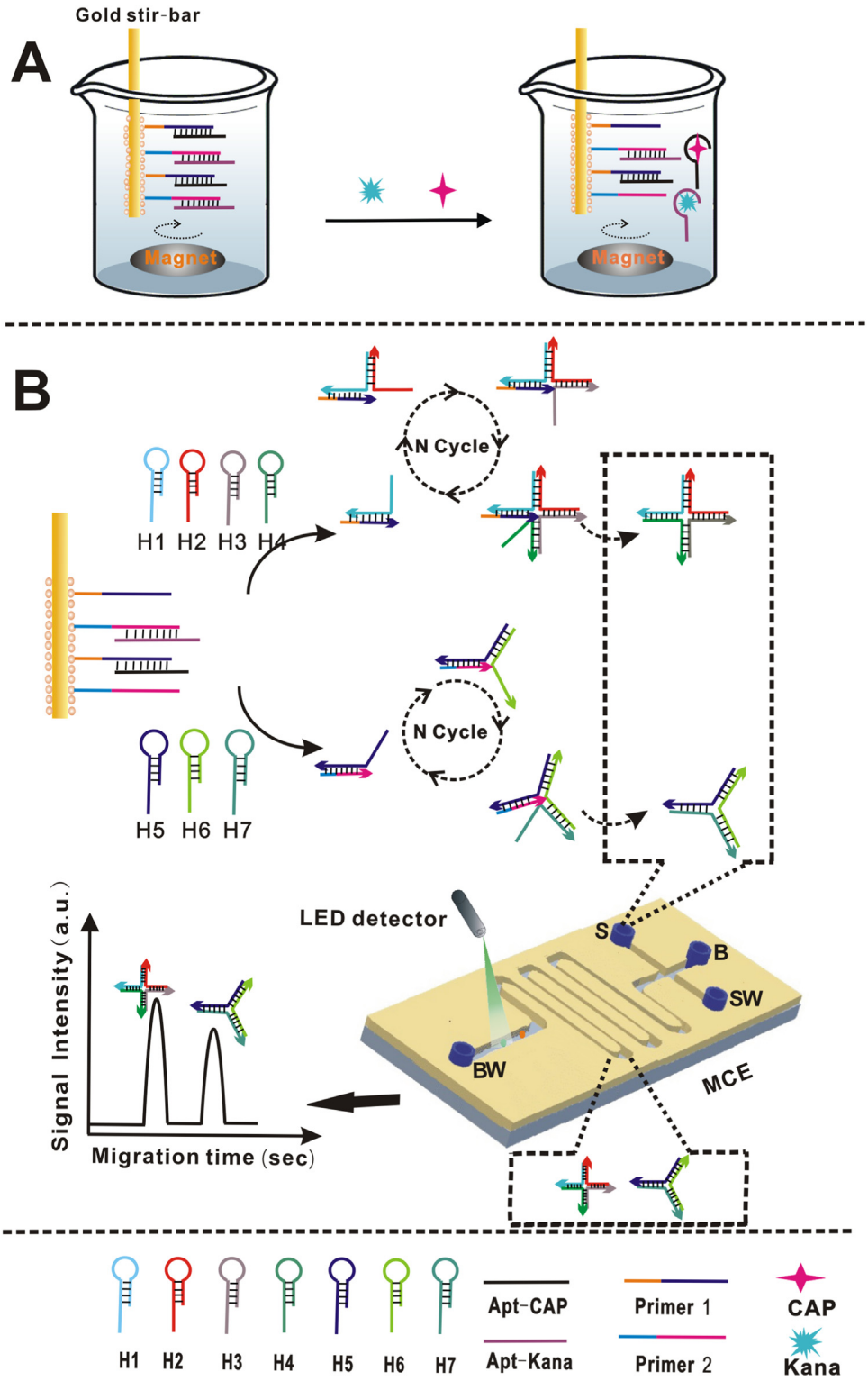

Scheme 1. Schematic illustration of the multiplexed aptasensor for antibiotics detection based on microchip electrophoresis and stir-bar assisted enzyme-free amplification. S: sample reservoir; B: buffer reservoir; SW: sample waste reservoir; BW: buffer waste reservoir.

supermarket in Ningbo, China. The process of CAP and Kana extraction was performed referencing the commercial ELISA kit for milk or fish samples and the detail procedure in the kit's protocol. The extraction process of CAP and Kana from the food was based upon the process of previous reported article (Takino et al., 2003). Firstly, 2 mL of extraction solution was used in reaction with the stir-bar functionalized with AuNPs-labeled hybridization probes at 25 °C for 1 h. After completion of the reaction, the gold bar was taken out and washed three times with deionized water. Next, the bar was placed into another PBS buffer. The buffer contained 0.4 μM hairpins (H1, H2, H3, H4, H5, H6 and H7 respectively). Finally, 50 μL reactions liquid were analyzed by Microchip electrophoresis system. ELISA was used for control experiment.

3. Results and discussion

3.1. Detection mechanism of the MCE based aptasensor

As illustrated in Scheme 1, the stir-bar assisted MAJR amplification strategy involved two kinds of encoded probes which included hybrid probes of CAP-apt/primer1 and Kana-apt/primer2. The probes were immobilized on gold bar by the way of Au-S interaction between the gold lattice and thiolated primers. In addition, the DNA hairpins (H1, H2, H3, H4, H5, H6 and H7) acted as raw materials to trigger MAJR for signal amplification. The MAJR process for signal amplification is shown in Scheme 1. In the presence of CAP and Kana, the functionalized stir-bar will bind with the targets to form CAP/CAP-aptamer and Kana/Kana-aptamer complex then released in supernatant. According to Stoltenburg's speculate, the stem structure of aptamers normally has a stabilizing function while the loop structures may assist in target binding (Stoltenburg et al., 2005). As a result, the primers (1 and 2) were exposed on the bar. Next, the stir-bar with the primers was placed in PBS buffer which contained 7 kinds of DNA hairpins. For the formation of the four-arm junction, 4 kinds of hairpins (H1, H2, H3 and H4) are included. By assisting of the corresponding primer 1, an assembly reaction was firstly occurred at the exposed toehold of H1 to generate an intermediate primer 1/H1. Then, the primer 1/H1 can open H2 to form the primer 1/H1/H2 hybrid. Subsequently, H3 and H4 were opened to form a DNA four-arm junction and released primer 1 again. The free primer 1 can catalyze the next assembly circle. In the same way, the primer 2 can catalyze three kinds of DNA hairpins (H5, H6 and H7) to form a three-arm branched junction and release primer 2 again. As a result, a large amount of three- and four-arm branched junctions were formed to amplify the signal by MCE. The charge-to-mass ratio of three- and four-arm branched junctions was different. Therefore, they can be separated and detected by MCE for quantification of Kana and CAP. After the stir-bar was taken out, 50 μL of reaction solution was injected in MCE system for automatic detection and analysis within 3 min. The signal of three- and four-arm branched junctions can be used to quantify the targets. In the absence of Kana and CAP, the primers were inhibited by the corresponding aptamers. Therefore, the cascade of assembly cannot be triggered and the hairpins can coexist in the system.

3.2. Characterization of the AuNPs, AuNPs modified aptamer (AuNPs-apt) and stir-bar functionalized with AuNPs -labeled aptamer

The functionalized stir-bar was characterized by the transmission electron microscopic (TEM), Scanning electron micrographs (SEM) and energy dispersive X-ray spectroscopy (EDX). As shown in Fig. 1A, the TEM image of AuNPs exhibited many spherical particles with average size about 25 nm. The UV–vis absorption spectra of AuNPs, primer probes, and AuNPs-primer are shown in Fig. 1B. The primers exhibited a characteristic peak at 258 nm (curve b) of DNA strands. The bare AuNPs showed a characteristic peak at 521 nm (curve c). After the primers labeling on the surface of AuNPs, the characteristic of absorption peaks at 258 nm and 521 nm are observed in curve a. It suggested that the primers were fixed on the AuNPs. The AuNPs on the surface of gold stir-bar was characterized by SEM. As shown in Fig. 1C, there were no AuNPs on the surface image of pure gold stir-bar. However, many AuNPs were observed on the bar after immobilization chemistry. It was indicated the successful immobilization of AuNPs on gold stir-bar. In addition, the pure gold stir-bar and aptamer functionalized gold stir-bar was characterized by EDX. The EDX of pure gold bar is shown in Fig. S2A. The main elements were C, N, O, S, Si and Au. After the DNA probes were immobilized on the gold stir-bar, a character peak of phosphorus (P) is observed in Fig. S2B. The peak of P could be attributed to the immobilization of DNA probes. All above results confirmed successful immobilization of primer onto the gold stir-bar. The UV–vis quantification experiment indicated that the quantity for primer 1 and primer 2 was 290 pmol cm^{-1} on the gold stir-bar (Fig. S3).

3.3. The feasibility of the MAJR strategy based on gel electrophoresis

To confirm if the multi-arm junctions were successfully fabricated and the feasibility of MAJR for signal amplification, a series of experiments based on gel electrophoresis were carried out. The ideal secondary structure of hairpins (H1, H2, H3, H4, H5, H6 and H7) is shown in Fig. S4. The concentration of all probes was 0.4 μM respectively. As shown in Fig. 2B, the bands of pure primer 1 and hairpins (H1, H2, H3 and H4) appeared in lane 1 and lane 2 respectively. When the hairpins of H1, H2, H3 and H4 were incubated with primer 1, a new band appeared in the Fig. 2B lane 3, which indicated that the primer 1 can trigger the MAJR to produce four-arm junctions. As shown in Fig. 2B, the bands corresponding to DNA probes of primer 2, and hairpins (H5, H6 and H7) appeared in lane 4 and lane 5, respectively. After primer 2 incubating with hairpins (H5, H6 and H7), a delayed band is observed (Fig. 2B lane 6). However, there was no new band to generate in lane 5. These results indicated that three-arm junctions formed successfully in the presence of primer 2 and the hairpins can coexist in the absence of primer. Interestingly, apart from the produce of the three- and four-arm junctions, there were many unknown bands in the Fig. 2B lane 3 and lane 6. We suspected that these bands could be the conjoined of hairpins such as primer1/H1/H2/H3, primer1/H1/H2, and primer1/H1 in lane 3; and the conjunctions of primer2/H5 and primer2/H5/H6 in lane 6. As shown in lane 7 of Fig. 2B, after the functionalized stir-bar reacted with 5 ng mL^{-1} Kana. The bar was placed in PBS which contains hairpins (H1, H2, H3, H4, H5, H6 and H7). A new band of three-arm junctions was observed, but there was on appeared of four-arm junctions in lane 7. Similarly, in the presence of 5 ng mL^{-1} CAP, only one new band of four-arm junctions occurred in lane 8. Notably, in the presence of 5 ng mL^{-1} Kana and CAP, both of the three- and four-arm junctions were appeared simultaneously in Fig. 2B lane 9. In addition, the MCE was used for testify if aptamer on the stir-bar can be released in presence of targets. If the probes on the stir-bar combined with target, the aptamer-target complex can be released from the stir-bar and separated by MCE for detection. The MCE image in the absence and presence of targets is shown in Fig. S5. There are two peaks corresponding to Kana and CAP aptamers in Fig. S5. These results demonstrated the feasibility of this method.

3.4. Optimization of detection condition

To achieve optimal sensing performance, several essential reaction conditions were optimized including (a) the hybridization bases between primers (primer 1 and primer 2) and aptamers (CAP-apt and Kana-apt); the incubation (b) time, (c) temperature and (d) pH of the gold bar with the targets; (e) stirring velocity of the magnetic beads.

The hybridization bases of primer 1 with CAP-apt and primer 2 with Kana-apt can influence the efficiency of aptamers capturing with targets. Therefore, a series of hybridization bases (10, 12, 14, 16 and 18 bp) were evaluated. As shown in Fig. S6, the high background signal is observed under 14 bp of hybridization bases between primer and aptamer. But the background signal was reduced significantly at 16 bp (Fig. S6A). On the basis of the largest signal to noise ratio, the optimum hybridization bases of 16 bp for primer 1/CAP-apt and primer 2/Kana-apt were selected for further experiments. To identify the optimal incubation time, the incubation time over a range from 10 to 80 min were examined (Fig. S6B). The signal rapidly increased from 10 to 60 min. According to these data, the optimum reaction time was considered as 60 min. As shown in Fig. S6C, the signal intensity steadily boosted with the increase of temperature from 10 °C to 25 °C and essentially plateaued at 30 °C. These results indicated the aptasensor can employ in a room temperature. As shown in Fig. S6D, the signal intensity gradually increased from pH 6.2 to pH 7.4 and reduced at pH values greater than 7.4. Therefore, the pH 7.4 was chosen for following experiment. In

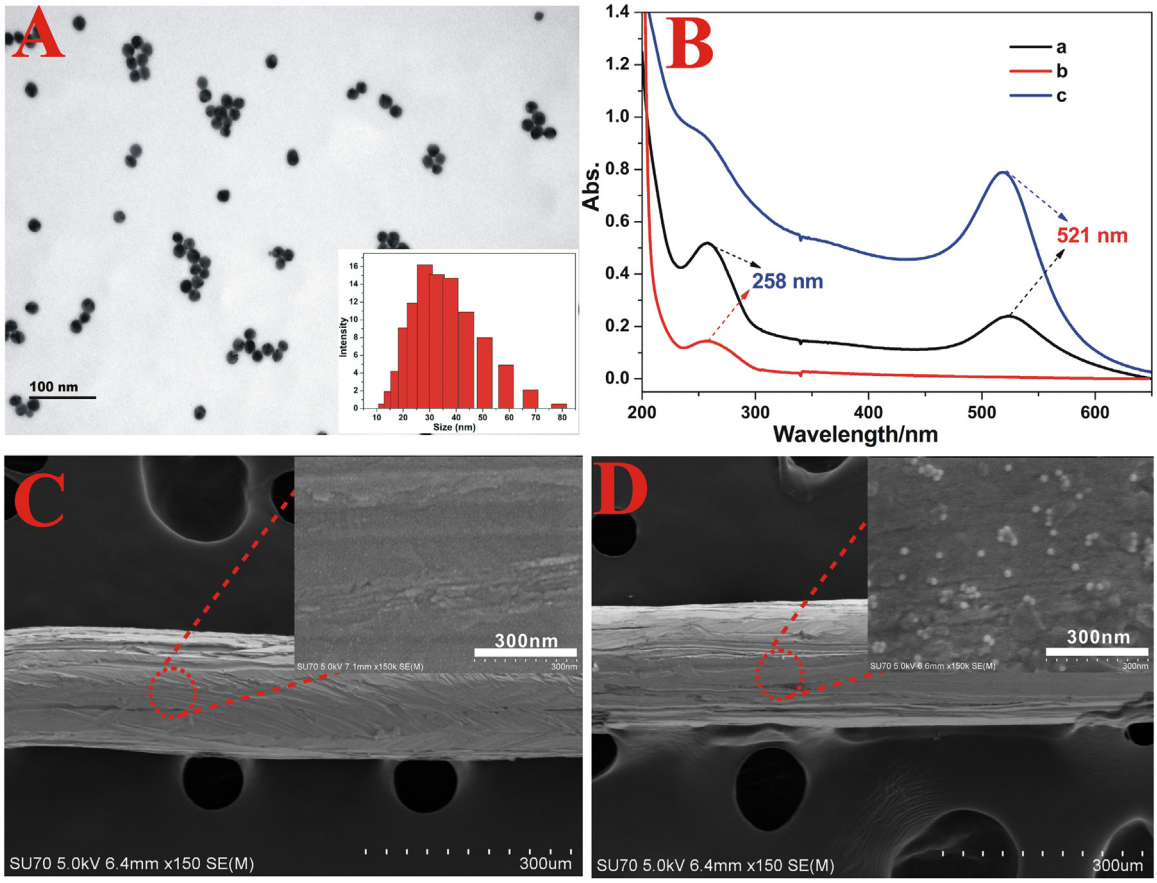

Fig. 1. (A) TEM image of AuNPs (the inset show its size distribution); (B) UV–vis spectra of AuNPs labeled primers (primer 1 and primer 2) (a), primer 1 and primer 2 (b), AuNPs (c); (C) SEM image of gold stir-bar (the inset show its surface); (D) SEM image of gold stir-bar (the inset shows the AuNPs uniform distribution in the surface of gold bar).

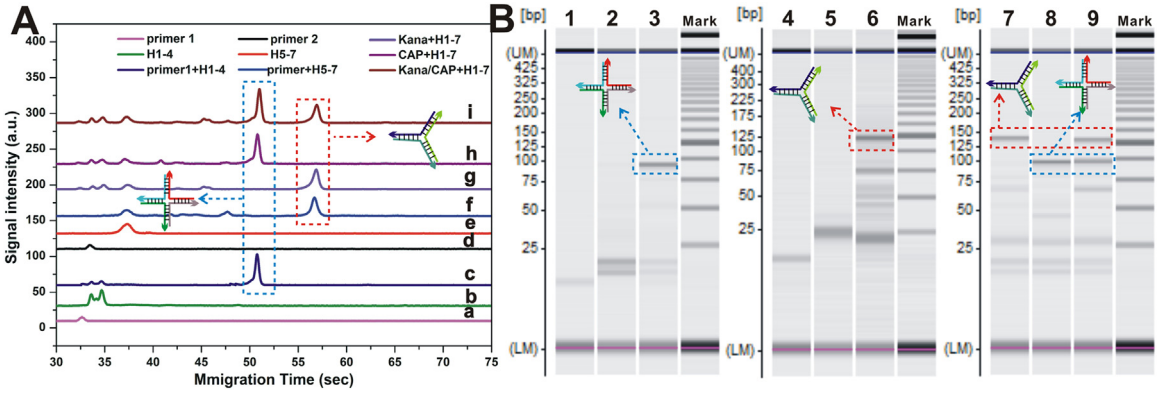

Fig. 2. (A) The feasibility of this method for Kana and CAP detection: (a) primer1 (b) the hairpins of H1, H2, H3 and H4; (c) primer1 + hairpins (H1, H2, H3 and H4); (d) primer2; (e) the hairpins of H5, H6 and H7; (f) primer2 + hairpins (H5, H6 and H7); (g) gold bar + 5 ng mL^{-1} Kana + hairpins (H1, H2, H3, H4, H5, H6 and H7); (h) gold bar + 5 ng mL^{-1} CAP + hairpins (H1, H2, H3, H4, H5, H6 and H7); (i) gold bar + 5 ng mL^{-1} Kana + 5 ng mL^{-1} CAP + hairpins (H1, H2, H3, H4, H5, H6 and H7). (B) The corresponding of gel electrophoresis image assay of the feasibility of this method. LM: Lower Marker; UM: Upper Marker.

addition, stirring velocity was also investigated. As shown in Fig. S6E, the signal reached to a plateau at 600 rpm. Therefore, the optimum stirring velocity was chosen to be 600 rpm.

3.5. Cross-reactivity of the system

In multiplex antibiotics detection, cross-reactivity of the analytes is a vital factor to evaluate the performance of a method. Therefore, a serious of experiments was carried out to investigate the method. As shown in Fig. S7a, the signal of CAP (0.01 ng mL^{-1}) was unaltered with the concentration of Kana from 0.01 to 10.0 ng mL^{-1}. In addition, the signal of Kana (0.01 ng mL^{-1}) was constant with the increasing amount of CAP from 0.01 to 10.0 ng mL^{-1} (Fig. S7b). Moreover, the simultaneous addition of CAP and Kana in a range from 0.01 to 10.0 ng mL^{-1} resulted in a simultaneous increase of both MCE signal (Fig. S7c). These results indicated that the cross-reactivity between the Kana and CAP was insignificant in this method.

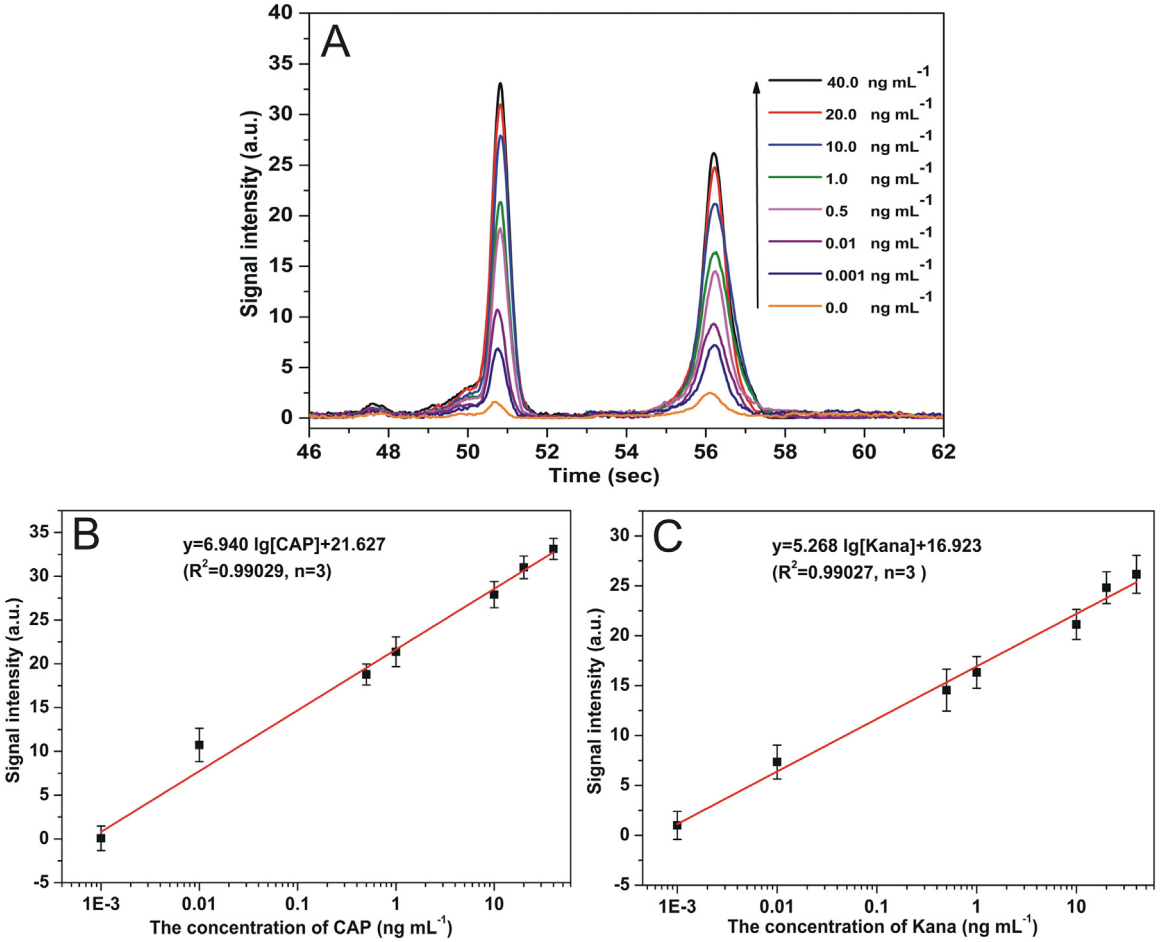

Fig. 3. (A) The MCE signal of the method in the presence of different concentrations of CAP and Kana in the range of 0.001–40 ng mL^{-1}. The calibration plots of the assay in the presence of different concentrations of CAP (B) and Kana (C), respectively.

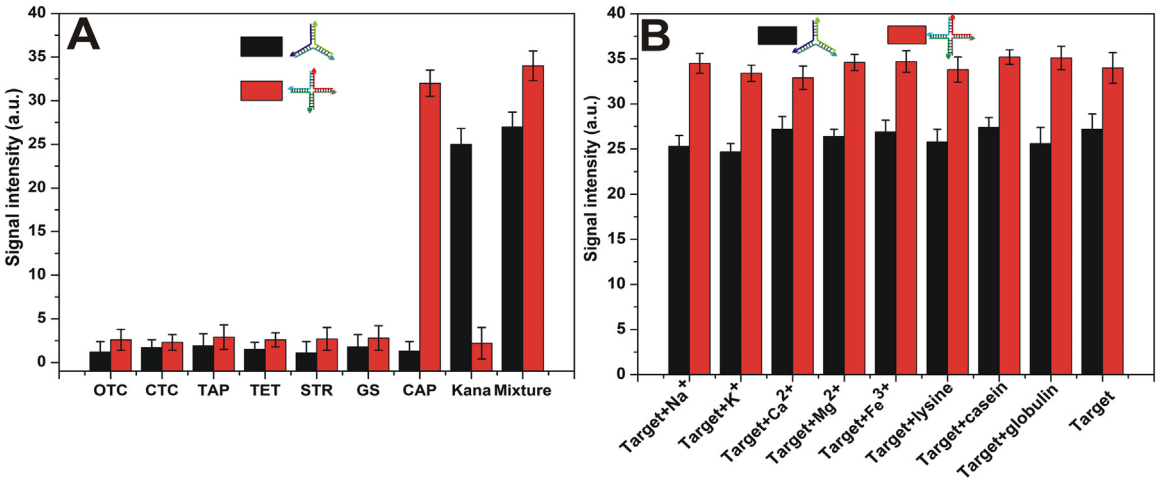

Fig. 4. (A) The selectivity of the method toward other antibiotics. (B) The interference of ions, amino acids and protein (the target contains 40 ng mL^{-1} of Kana and CAP respectively).

3.6. The detection of CAP and Kana

To investigate the analytical performance of the universal MCE system, different concentrations of CAP and Kana were analyzed under the optimum conditions. As shown in Fig. 3A, the signal of three-arm junction and four-arm junction raised with the increase of Kana and CAP concentration respectively. The calibration curves displayed a good linear relationships in the range from 0.001 to 40 ng mL^{-1} with a regression equation of y = 6.940 lg [CAP] + 21.672 (R^2 = 0.99029, n = 3) and y = 5.268 lg [Kana] + 16.923 (R^2 = 0.99027, n = 3). The limit of detection (LOD) was 0.52 pg mL^{-1} for CAP and 0.41 pg mL^{-1} for Kana, respectively. The results indicated that the multiplexed aptasensor displayed high sensitivity. Moreover, some reported methods for Kana detection was listed in Table S3 for comparison of the

Table 1
The developed method and ELISA method for CAP and Kana detection (n = 5).

Target	Samples	Background (ng mL^{-1})	Added (ng mL^{-1})	Detection (ng mL^{-1})	ELISA (ng mL^{-1})	Recovery (%)	RSD (%)
CAP	Milk1	0.007	0.005	0.013 ± 0.004	0.015 ± 0.003	108.3	4.7
	Milk2	ND	0.05	0.048 ± 0.002	0.051 ± 0.005	96.0	6.8
	Milk3	0.012	5.0	5.052 ± 0.043	5.037 ± 0.031	100.8	4.1
	Fish1	ND	0.005	0.0047 ± 0.006	ND	94.0	6.2
	Fish2	ND	0.05	0.046 ± 0.005	0.051 ± 0.002	92.0	5.8
	Fish3	0.013	5.0	5.024 ± 0.016	5.072 ± 0.064	100.2	3.6
Kana	Milk1	ND	0.005	0.0049 ± 0.002	ND	98.0	3.2
	Milk2	0.009	0.05	0.061 ± 0.009	0.056 ± 0.011	103.3	5.1
	Milk3	ND	5.0	5.014 ± 0.017	4.952 ± 0.057	100.3	4.3
	Fish1	ND	0.005	0.0056 ± 0.0007	ND	112.0	6.2
	Fish2	ND	0.05	0.053 ± 0.006	0.061 ± 0.008	106.0	5.4
	Fish3	0.016	5.0	5.043 ± 0.036	5.002 ± 0.019	100.5	4.9

ND: not detected.

detection performance.

3.7. Specificity and reproducibility of the method

The specificity is important to evaluate the assay. Therefore, the interference of coexisting antibiotics, ions and amino acids was studied. In Fig. 4A, when six other antibiotics (OTC, CTC, TAP, TET, STR and GS) reached 2 times the CAP and Kana concentration (40 ng mL^{-1}), only CAP and Kana were generated the signals, which indicated that the method had a good specificity and selectively to CAP and Kana. In Fig. 4B, the interference experiment on metal ions (400 ng mL^{-1} Na^+, K^+, Ca^{2+}, Mg^{2+} and Fe^{3+}), amino acid (400 ng mL^{-1}lysine) and proteins (400 ng mL^{-1}casein and globulin) were carried out under CAP and Kana concentration (40 ng mL^{-1}). However, the change in the MCE signal was less than 4.5%, which indicated that this interference had negligible effects on the assay of CAP and Kana in this MCE system.

The reproducibility of the universal MCE system was investigated by the relative standard deviation (RSD) of intra- and inter-assays. It was implemented by detecting the mixture 20 ng mL^{-1} of CAP and Kana in PBS buffer (10 nM, pH = 7.4) under the optimal conditions. The RSDs of CAP and Kana were 4.23% and 5.74% for inter-assay respectively, and 8.6% and 9.8% for intra-assay respectively. It indicated that this universal MCE system had a good reproducibility.

3.8. The assay performance

The applicability of the multiple aptasensor based on universal MCE system in actual sample was investigated by several milk and fish samples under the optimum experimental conditions. The standard addition method was used to determine the recovery rate. As shown in Table 1, the recoveries from milk and fish samples were between 96.0–108.3% and 90.2–100.2%, respectively for CAP; 98.0–103.3% and 100.5–112.0%, respectively for Kana. The results were in agreement with the ELISA method. It indicated the universal MCE system can be used to detect CAP and Kana in milk and fish samples.

4. Conclusion

In this study, a highly -sensitive and -selective multiplexed aptasensor based on a universal double-T MCE chip was developed for one step, simultaneously detect CAP and Kana in food samples. Benefiting from the used of stir-bar, the matrix interference was obviously eliminated. In addition, the enzyme-free of DNA multi-arm junction self-assembled recycling (MAJR) can largely improve the sensitivity and simplify the detection process. However, the assay appeared some limitations as well. For examples, numerous hairpins probes were needed for MAJR. In the study, 7 kinds of hairpins are needed to detect two targets. Thus, if the assay were employed to detect more targets, a large number of hairpins were required. This will make the measurement process more sophisticated. For the future improvement, the design and categories of hairpins should be simplified to detect more targets simultaneously. Above all, the assay can be considered a potential screening method for detecting different antibiotic residues simultaneously in food.

CRediT authorship contribution statement

Kai Zhang: Investigation, Conceptualization, Writing - review & editing, Methodology, Data curation. **Ning Gan:** Supervision, Data curation, Conceptualization, Validation, Writing - review & editing, Data curation. **Zhipeng Shen:** Methodology, Data curation. **Jinxuan Cao:** Software, Writing - review & editing, Validation, Supervision. **Futao Hu:** Writing - review & editing. **Tianhua Li:** Writing - review & editing.

Acknowledgments

This work was supported by National Key R&D Program of China (No. 2016YFD0401502), the National Natural Science Foundation of China (No. 11832013, No. 31871825), Natural Science Foundation of Zhejiang (LY19B050001, LY17C200007), Zhejiang Province Welfare Technology Applied Research Project (2017C33004, LGC19B070003, LGN18H300001), Zhejiang Provincial Top Key Discipline of Biology (ZS2015005), the Guangdong Provincial Key Laboratory of Environmental Pollution and Health (No. GDKLEEH201807), the Natural Science and Huiming Foundation of Ningbo (2016A610084, 2017A610225, 2017C50035) and K. C. Wong Magna Fund in Ningbo University.

Declaration of interests

The authors declare that they have no known competing financial interests or personal relationships that could have appeared to influence the work reported in this paper.

Appendix A. Supplementary material

Supplementary data associated with this article can be found in the online version at https://doi.org/10.1016/j.bios.2019.01.044.

References

Bi, S., Xiu, B., Ye, J., Dong, Y., 2015. Target-catalyzed DNA four-way junctions for CRET imaging of microRNA, concatenated logic operations, and Self-assembly of DNA nanohydrogels for targeted drug delivery. Acs Appl. Mater. Interfaces 7 (41), 23310–23319.

Conzuelo, F., Campuzano, S., Gamella, M., Pinacho, D.G., Reviejo, A.J., Marco, M.P., Pingarrón, J.M., 2013. Integrated disposable electrochemical immunosensors for the simultaneous determination of sulfonamide and tetracycline antibiotics residues in milk. Biosens. Bioelectron. 50 (24), 100–105.

Dincer, C., Bruch, R., Kling, A., Dittrich, P.S., Urban, G.A., 2017. Multiplexed point-of-care testing – xPOCT. Trends Biotechnol. 35 (8), 728–742.
Ellington, A.D., Szostak, J.W., 1990. In vitro selection of RNA molecules that bind specific ligands. Nature 346 (6287), 818–822.
Gao, H., Pan, D., Gan, N., Cao, J., Sun, Y., Wu, Z., Zeng, X., 2015. An aptamer-based colorimetric assay for chloramphenicol using a polymeric HRP-antibody conjugate for signal amplification. Microchim. Acta 182 (15–16), 2551–2559.
García, C.D., Henry, C.S., 2003. Direct determination of carbohydrates, amino acids, and antibiotics by microchip electrophoresis with pulsed amperometric detection. Anal. Chem. 75 (18), 4778–4783.
Gaudin, V., 2017. Advances in biosensor development for the screening of antibiotic residues in food products of animal origin - a comprehensive review. Biosens. Bioelectron. 90, 363–377.
Kotani, S., Hughes, W.L., 2017. Multi-arm junctions for dynamic DNA nanotechnology. J. Am. Chem. Soc. 139 (18), 6363.
Lili, W., Jing, W., Qin, W., Chonghui, H., Lei, Z., Jing, W., Qiaosheng, P., 2012. Rapid and sensitive determination of sulfonamide residues in milk and chicken muscle by microfluidic chip electrophoresis. J. Agric. Food Chem. 60 (7), 1613–1618.
Lu, H., Yuan, G., He, Q., Chen, H., 2009. Rapid analysis of anthracycline antibiotics doxorubicin and daunorubicin by microchip capillary electrophoresis. Microchem. J. 92 (2), 170–173.
Manz, A., Graber, N., Widmer, H.M., 1990. Miniaturized total chemical analysis systems: a novel concept for chemical sensing. Sens. Actuators B Chem. 1 (1), 244–248.
Martín, A., Vilela, D., Escarpa, A., 2012. Food analysis on microchip electrophoresis: an updated review. Electrophoresis 33 (15), 2212–2227.
Nantana, N., Worapot, S., Lunte, S.M., Leena, S., 2015. Recent applications of microchip electrophoresis to biomedical analysis. J. Pharm. Biomed. Anal. 113, 72–96.
Oertel, R., Neumeister, V., Kirch, W., 2004. Hydrophilic interaction chromatography combined with tandem-mass spectrometry to determine six aminoglycosides in serum. J. Chromatogr. A 1058 (1), 197–201.
Shih, T.T., Lee, H.L., Chen, S.C., Kang, C.Y., Shen, R.S., Su, Y.A., 2018. Rapid analysis of traditional Chinese medicine Pinellia ternata by microchip electrophoresis with electrochemical detection. J. Sep. Sci. 41 (3), 740–746.
Song, K.-M., Cho, M., Jo, H., Min, K., Jeon, S.H., Kim, T., Han, M.S., Ku, J.K., Ban, C., 2011. Gold nanoparticle-based colorimetric detection of kanamycin using a DNA aptamer. Anal. Biochem. 415 (2), 175–181.
Spindel, S., Sapsford, K.E., 2014. Evaluation of optical detection platforms for multiplexed detection of proteins and the need for point-of-care biosensors for clinical use. Sensors 14 (12), 22313–22341.
Stoltenburg, R., Reinemann, C., Strehlitz, B., 2005. FluMag-SELEX as an advantageous method for DNA aptamer selection. Anal. Bioanal. Chem. 383 (1), 83–91.
Suárez, G., Jin, Y.H., Auerswald, J., Berchtold, S., Knapp, H.F., Diserens, J.M., Leterrier, Y., Månson, J.A., Voirin, G., 2009. Lab-on-a-chip for multiplexed biosensing of residual antibiotics in milk. Lab A Chip 9 (11), 1625–1630.
Sun, Y., Ren, Q., Liu, B., Qin, Y., Zhao, S., 2016. Enzyme-free and sensitive electrochemical determination of the FLT3 gene based on a dual signal amplified strategy: controlled nanomaterial multilayers and a target-catalyzed hairpin assembly. Biosens. Bioelectron. 78, 7–13.
Takino, M., Daishima, S., Nakahara, T., 2003. Determination of chloramphenicol residues in fish meats by liquid chromatography–atmospheric pressure photoionization mass spectrometry. J. Chromatogr. A 1011 (1), 67–75.
Tuerk, C., Gold, L., 1990. Systematic evolution of ligands by exponential enrichment: RNA ligands to bacteriophage T4 DNA polymerase. Science 249 (4968), 505–510.
Wang, B., Zhou, X., Yao, D., Sun, X., He, M., Wang, X., Yin, X., Liang, H., 2017a. Contribution of gold nanoparticles to the catalytic DNA strand displacement in leakage reduction and signal amplification. Chem. Commun. 53 (79), 10950–10953.
Wang, Y., Gan, N., Zhou, Y., Li, T., Hu, F., Cao, Y., Chen, Y., 2017b. Novel label-free and high-throughput microchip electrophoresis platform for multiplex antibiotic residues detection based on aptamer probes and target catalyzed hairpin assembly for signal amplification. Biosens. Bioelectron. 97, 100–106.
Wen, Y., Jiang, J., Cai, D., Zhao, P., Liao, J., Ge, S., 2016. Ultrasensitive visual detection of DNA with tunable dynamic range by using unmodified gold nanoparticles and target catalyzed hairpin assembly amplification. Biosens. Bioelectron. 77, 421–427.
Yang, D., Tang, Y., Miao, P., 2017. Hybridization chain reaction directed DNA superstructures assembly for biosensing applications. Trac Trends Anal. Chem. 94, 1–13.
Ye, F., Shi, M., Huang, Y., Zhao, S., 2010. Noncompetitive immunoassay for carcinoembryonic antigen in human serum by microchip electrophoresis for cancer diagnosis. Clin. Chim. Acta 411 (15), 1058–1062.
Zhang, K., Gan, N., Hu, F., Chen, X., Li, T., Cao, J., 2018. Microfluidic electrophoretic non-enzymatic kanamycin assay making use of a stirring bar functionalized with gold-labeled aptamer, of a fluorescent DNA probe, and of signal amplification via hybridization chain reaction. Microchim. Acta 185 (3), 181.
Zhihe, Q., Xiaoxiao, H., Jin, H., Kemin, W., Zhen, Z., Taiping, Q., Zhengui, M., Hui, S., Dinggeng, H., 2014. Target-catalyzed dynamic assembly-based pyrene excimer switching for enzyme-free nucleic acid amplified detection. Anal. Chem. 86 (10), 4934–4939.
Zhou, L., Gan, N., Hu, F., Li, T., Cao, Y., Wu, D., 2018a. Microchip electrophoresis array-based aptasensor for multiplex antibiotic detection using functionalized magnetic beads and polymerase chain reaction amplification. Sens. Actuators B Chem. 263, 568–574.
Zhou, L., Gan, N., Wu, Y., Hu, F., Lin, J., Cao, Y., Wu, D., 2018b. Multiplex detection of quality indicator molecule targets in urine using programmable hairpin probes based on a simple double-T type microchip electrophoresis platform and isothermal polymerase-catalyzed target recycling. Analyst 143, 2696–2704.